Appl Phys B (2008) 93: 183–187
DOI 10.1007/s00340-008-3180-6

Applied Physics B
Lasers and Optics

Enhanced evanescent coupling to whispering-gallery modes due to gold nanorods grown on the microresonator surface

S.I. Shopova · C.W. Blackledge · A.T. Rosenberger

Received: 4 June 2008 / Published online: 28 August 2008

Abstract The evanescent fields of whispering-gallery modes of a high-Q dielectric microresonator are locally enhanced via excitation of the surface plasmon resonances of gold nanorods grown on the microresonator's surface. This results in enhanced coupling between the microresonator and an adjacent tapered optical fiber for frequencies in the vicinity of the surface plasmon resonance. The experimental results presented here demonstrate coupling enhancement by a factor of 100–1000, accompanied by an increase in absorption and scattering loss that is very small by comparison.

PACS 42.60.Da · 73.27.Lp · 81.07.Bc

1 Introduction

Free charge oscillations at the interface of a metal and a dielectric, surface plasmons (SPs), can be excited optically. At the surface of a metal film, SPs can be excited by evanescent waves or near fields produced from plane waves by a prism [1, 2], a grating structure [3–5], or random surface roughness [6]. Applications of the evanescent field of a waveguide for the resonant excitation of SPs are described extensively in the literature [7, 8]. The presence of a metal layer on the waveguide surface converts the waveguide mode into a waveguide-surface plasmon coupled mode, greatly enhancing the evanescent field [9]. Such structures are used as sensors because they can combine the SP-enhanced evanescent field with simple surface functionalization techniques [9, 10]. The sensitivity of waveguide-surface plasmon coupled sensors can be further optimized by using metal nanoparticles deposited on the surface instead of a thin metal film [10, 11], because the conditions for SP excitation are less restrictive for nanoparticles than for thin films, and the field enhancement is greater. Another advantage can be gained by using rod-shaped nanoparticles: the ability to tailor the spectral position of the surface plasmon resonance by controlling the aspect ratio (length to width) of the nanorods (NRs) [12].

Here we report experimental investigations of the optical response of a system in which SPs are coupled to the whispering-gallery modes (WGMs) of a fused-silica microsphere, providing compound resonant enhancement. Applying the advantages mentioned above, we do not use a small sphere coated with a solid metal film as in [13], but a sphere a few hundred μm in diameter with well-separated gold NRs grown on its surface. In such a sphere, a WGM can be efficiently excited by tapered-fiber coupling, and the SP resonances of the Au NRs can be excited by the WGM's evanescent field. Localized enhancement of the evanescent field caused by resonant excitation of the SPs enhances the coupling of light between the resonator and the tapered fiber. By monitoring the resonance dips in the fiber throughput before and after growing gold NRs on the microresonator surface, we can estimate the induced changes in coupling (tunneling probability of a photon from the fiber mode to a WGM or vice versa) as well as in scattering and absorption loss. Our measurements show coupling enhancement by a factor in the 100–1000 range, accompanied by very little

S.I. Shopova
Biological Engineering Department, University of Missouri, Columbia, MO 65211, USA

C.W. Blackledge · A.T. Rosenberger (✉)
Department of Physics, Oklahoma State University, Stillwater, OK 74078-3072, USA
e-mail: atr@okstate.edu
Fax: +1-405-7446811

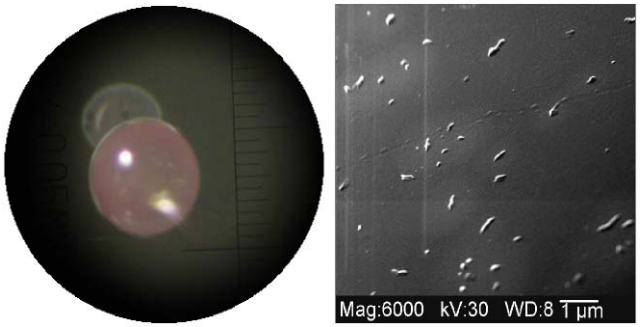

a b

Fig. 1 (**a**) Microsphere coated with Au nanorods and nanospheres. The smallest division on the scale is 50 μm. The image in back is a reflection. (**b**) Scanning electron micrograph of a portion of the surface of a coated microsphere, showing a distribution of nanoparticle sizes and shapes

increase in scattering and absorption loss (less than a factor of 3). The small increase in scattering and absorption is in accord with previous calculations [14]. These NR-coated microresonators could provide sensitivity enhancement in various types of chemical sensors.

2 Gold nanorod growth

Permanent attachment of gold nanorods directly on the surface of a high-quality optical microresonator, with controllable areal density, is achieved using the growth technique described in [15]. Gold nanoparticles are nucleated using thioglycolic acid-capped HgTe nanoparticle seeds adsorbed to a polyelectrolyte intermediary layer on the microsphere's surface. Of the gold nanoparticles grown, about 30% are rod-shaped with aspect ratios between 3 and 5, and about 70% are approximately spherical. Before its surface is coated, the initial quality factor Q of a bare resonator at a wavelength of 830 nm is typically a few times 10^8. After NR growth, the Q is reduced but is still on the order of 10^6 if the nanoparticles (nanorods and nanospheres) constitute only a fraction of a monolayer. Figure 1(a) is a photograph of a 450-μm-diameter sphere. The gold nanoparticles on the surface are responsible for the pale pink color. Figure 1(b) shows a scanning electron micrograph of the surface of a microsphere coated with gold nanoparticles. These are typical of the coated microspheres used in the coupling enhancement experiments reported below. The NRs measure 30–70 nm in width and 120–300 nm in length.

3 Experimental results

A simplified schematic of the setup is shown in Fig. 2. Light from a cw laser (Ti:sapphire with a wavelength tunable from

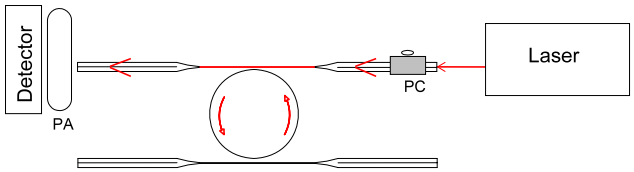

Fig. 2 Light (polarization controlled by PC and analyzed by PA) is evanescently coupled to the WGMs of a microresonator on which Au NRs have been grown. The second fiber is brought into contact with the microsphere to probe the coupling regime of the resonator mode

780 to 850 nm or diode with a wavelength tuned around 1550 nm) is launched into a single-mode optical fiber that is tapered for coupling. The polarization incident on the microresonator can be selected by a polarization controller (PC), and a polarization analyzer (PA) reads the polarization of the light coupled back to the fiber. From the tapered part of the fiber, light is evanescently coupled to the WGMs of the microresonator. As the input light is scanned in frequency, dips in the detected throughput correspond to WGM resonances. The WGMs are classified by the ratio $x = T/\alpha L$ of coupling loss T (probability of photon tunneling from WGM to fiber mode) to intrinsic loss αL (due to absorption and scattering), where α is the intrinsic loss coefficient and L is the microresonator circumference. A WGM with $x > 1$ is referred to as overcoupled, and one with $x < 1$ is called undercoupled. The loss ratio x determines the relative dip depth (also called extinction ratio) M_0 [16],

$$M_0 = \frac{4x}{(1+x)^2}, \tag{1}$$

which is maximum ($M_0 = 1$, and throughput goes to zero) for critical coupling ($x = 1$).

Because a measured dip depth M_0 does not uniquely determine the loss ratio x, it is necessary to have a method for determining the coupling regime (undercoupled or overcoupled). Bringing a second fiber close to the microsphere effectively increases the intrinsic loss, changing the first fiber's throughput dip depth. Adding some extra loss makes the dip of an overcoupled mode deeper (M_0 increases), and that of an undercoupled mode shallower (M_0 decreases). With the knowledge of whether x is less than or greater than one, x can be uniquely determined from the measured M_0.

Microspheres ranging between 400 and 700 μm in diameter were used for investigating the effect of SP-enhanced evanescent fields on the coupling to WGMs using a 2.5-μm-diameter tapered fiber. The laser wavelength was scanned several GHz around 830 nm to display a number of WGM resonance dips in the fiber throughput. Using the second fiber, we noted that the observed modes of a bare sphere will usually be distributed throughout the coupling regimes. After coating the microsphere resonator with a polyelectrolyte layer (poly(diallyldimethylammonium chloride), or PDDA),

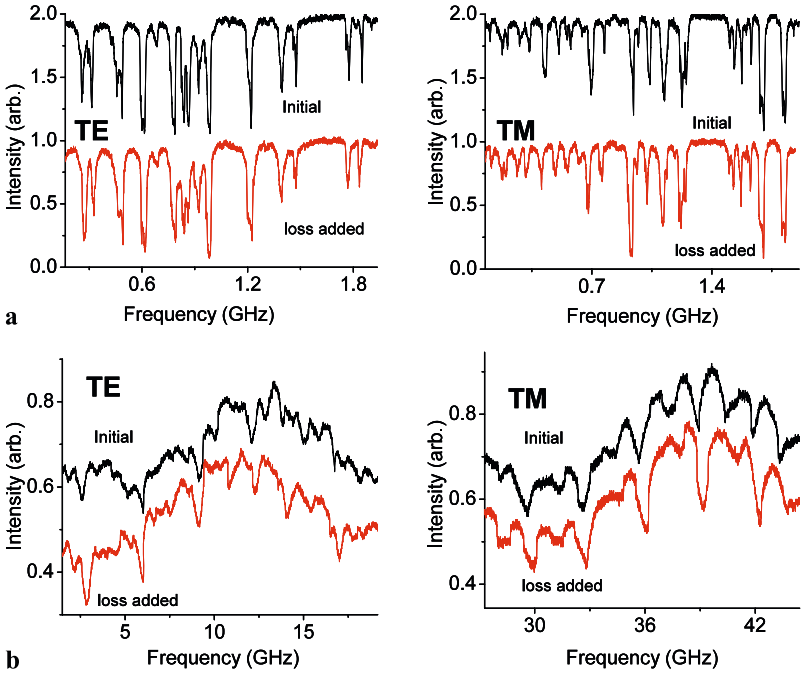

Fig. 3 Fiber throughput power showing dips corresponding to TE and TM WGMs of (**a**) a microsphere coated with a PDDA monolayer, and (**b**) the same microsphere after growing Au nanorods and nanospheres on its surface. In all plots, zero on the *vertical axis* indicates the baseline of intensity for the "loss added" traces; a dip with $M_0 = 1$ would go to zero. All "initial" traces have been displaced upward for clarity: (**a**) by 1.0; (**b**) by 0.1. Only the relative frequency on the *horizontal axes* is relevant; the wavelength is near 830 nm

it was tested with the second fiber again. The additional absorption and scattering losses introduced by the PDDA increase the intrinsic loss by about an order of magnitude. Therefore, the PDDA-coated microresonator coupled to the same tapered fiber (under similar coupling conditions—fiber and sphere in contact) resulted in predominantly undercoupled modes. This is seen in Fig. 3(a), where adding the second-fiber loss makes the dips shallower. In actuality, the coupling fiber diameter was chosen to ensure undercoupling for the PDDA-coated sphere. After growing gold NRs on the surface of the same resonator, the coupling regime was tested again using the second fiber. As Fig. 3(b) shows, nearly all the modes became strongly overcoupled, as the addition of loss makes the dips deeper. This transition from undercoupled to overcoupled is evidence of coupling enhancement, and Fig. 3 shows that this enhancement is seen for both WGM polarizations, TE (electric field essentially orthogonal to the microsphere radius) and TM (electric field essentially parallel to the microsphere radius).

Comparing the fiber throughput dips of the microresonator with Au NRs to those of the same resonator with just the PDDA coating before growing NRs, we find the following, as shown in the next section. The localized SP enhancement of the evanescent WGM field results in an enhancement of the coupling, as measured by the tunneling probability T, by a factor that is most likely between 100 and 1000. At the same time, the intrinsic scattering and absorption loss, αL, increases by a factor that is probably not greater than 3.

Further evidence that SP excitation on gold NRs is responsible for the observed coupling enhancement is shown below. The TE-polarized WGMs of another microsphere coated with PDDA showed undercoupled behavior at wavelengths of 800 and 1550 nm. Figure 4 shows the WGM spectra of that resonator, after Au nanoparticles were grown on its surface, at the two wavelengths. It is seen that, whereas the 800-nm modes are now strongly overcoupled, as in Fig. 3(b), the 1550-nm modes remain undercoupled, indicating much less coupling enhancement than at 800 nm.

The wavelength dependence of the coupling enhancement indicates that it is probably caused by the SP-related enhancement of the local evanescent fields. This conclusion is supported by calculations and results that suggest a strong longitudinal SP resonance of the NRs somewhat above 800 nm but well below 1550 nm [17]. This longitudinal SP resonance lies just beyond the wavelength range of our earlier report [15]. The exact longitudinal resonance wavelength depends on the NR aspect ratio, whereas the transverse SP resonance of the NRs remains near 530 nm, along with the nanospheres' SP resonance.

4 Analysis

The enhancement factors for coupling and intrinsic loss can be found from measurements made on traces such as those shown in Fig. 3. Measurements of the depth and width of a dip give the quality factor Q and loss ratio x for that mode, provided that the coupling regime is known. Knowing Q and x before and after Au NR growth is sufficient to determine both enhancement factors. To see this, consider the follow-

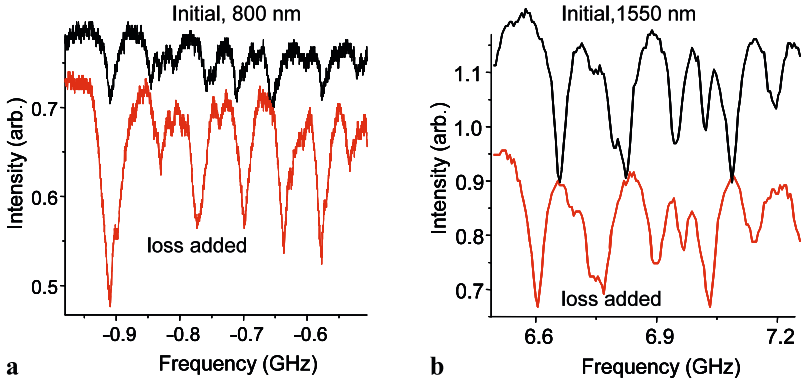

Fig. 4 TE WGMs of a sphere, with Au nanorods and nanospheres grown on its surface, at two different wavelengths: (**a**) 800 nm; (**b**) 1550 nm

ing expressions for the total (or loaded, i.e., including coupling loss T) Q of a WGM:

$$Q = \frac{\nu}{\Delta\nu} = \frac{2\pi n_{\text{eff}} L}{\lambda(T + \alpha L)}, \tag{2}$$

where ν is the WGM frequency, $\Delta\nu$ the mode width, n_{eff} the effective index of refraction of the mode, L the microresonator circumference, λ the vacuum wavelength, and α the intrinsic loss coefficient. Note that $\Delta\nu$ and Q^{-1} are proportional to the total loss $T + \alpha L$; defining the coupling and intrinsic quality factors, Q_c and Q_i, to be similarly inversely proportional to T and αL, respectively, we have $Q^{-1} = Q_c^{-1} + Q_i^{-1}$. Using the definition of the loss ratio, $x = T/\alpha L$, gives

$$\begin{aligned} Q_c &= Q\left(1 + \frac{1}{x}\right), \\ Q_i &= Q(1 + x). \end{aligned} \tag{3}$$

Now the coupling enhancement factor can be found by comparing coupling losses before (T') and after (T'') growing Au NRs on the surface of the resonator:

$$F_c = \frac{T''}{T'} = \frac{Q_c'}{Q_c''} = \frac{Q'(1 + \frac{1}{x'})}{Q''(1 + \frac{1}{x''})}, \tag{4}$$

and a similar ratio of the intrinsic losses before and after gives the intrinsic loss enhancement:

$$F_i = \frac{\alpha'' L}{\alpha' L} = \frac{Q_i'}{Q_i''} = \frac{Q'(1 + x')}{Q''(1 + x'')}. \tag{5}$$

Note that the coupling enhancement given by (4) is not the same as a previously reported enhancement in extinction ratio [18]. The two will be compared in more detail below.

Expressions (4) and (5) for the enhancement factors implicitly assume that n_{eff} is not changed by the addition of NRs. However, any process that significantly affects the evanescent fraction of a WGM will change its effective index; since the evanescent portion makes up only a fraction of a percent of the mode volume, the change in n_{eff} is unlikely to be more than a few percent, which may be neglected in the ratios in (4) and (5) because of the uncertainty in the estimation of the enhancement factors. The change in n_{eff} contributes to that uncertainty in another way, however; a small change in effective index means that each mode will significantly shift in frequency, and thus it is not possible to identify a mode observed after adding NRs with the same mode observed before.

Even though this means that the enhancement factors for a given mode cannot be calculated unambiguously, and though the enhancement will vary somewhat from mode to mode because the evanescent fraction does, a reasonably reliable estimate can still be found for the range of each enhancement factor. Since, as seen in Fig. 3 and in similar observations not reported in detail here, the modes go from being very predominantly undercoupled before to very predominantly overcoupled after adding NRs, one can use a "typical" mode for making estimates. Furthermore, the coupling enhancement found in this way will be an underestimate because we assume that some of the "after" modes of Fig. 3(b) are the same as some of the "before" modes of Fig. 3(a). Modes that are too strongly undercoupled before or too strongly overcoupled after will not be observed because their dips will be too shallow; by discounting the possibility of unobserved modes transforming under NR addition into observed ones, or vice versa, our coupling enhancement estimates will not be as large as they might be otherwise.

In Fig. 3(a), before adding NRs, the WGM parameters have the following ranges: Q', 1.5×10^7–4.5×10^7; M_0', 0.15–0.80; x', 0.04–0.40. After, in Fig. 3(b), the ranges are: Q'', 7.5×10^5–3.0×10^6; M_0'', 0.04–0.15; x'', 25–100. Assuming the enhancement is not too much different for different modes, dips that are relatively shallow before NR growth should correspond to deep dips after, and vice versa. For example, if we assume that Q drops by a factor of 30 as a dip goes from the deep limit before to the shallow limit after, we find $F_c = 750$ and $F_i = 1.2$. On the other hand, assuming a Q ratio of 60 as the dip goes from the shallow

limit to the deep limit gives $F_c = 210$ and $F_i = 0.84$. Other choices, some less physically justifiable, give a range of F_c from about 100 to about 1500, and a range of F_i from 0.21 to 3.2. If we argue that adding NRs is unlikely to *decrease* scattering and absorption losses, F_i should be greater than 1.0, and this restricts the range of F_c to roughly 100–1000.

5 Conclusions

In summary, it is shown that synthesis of Au NRs on the surface of a high-Q microsphere leads to an increase in evanescent coupling between the microresonator and a tapered optical fiber. The coupling, as measured by the probability of tunneling between fiber mode and WGM, is enhanced by a factor whose lower limit is most likely between 100 and 1000. At the same time, the intrinsic scattering and absorption loss increases by a factor that is probably not greater than 3. This coupling enhancement is a result of the surface plasmon resonance enhancement of the localized evanescent WGM field, because it is evident at 830 nm, near the longitudinal plasmon resonance of the NRs, but absent at the far-detuned wavelength of 1550 nm.

These results are different in several respects from the previously reported coupling enhancement to the WGMs of a cylinder provided by a prism coated with a gold film lying between the prism and the microresonator [18]. Using nanoparticles to provide the SP evanescent-wave enhancement makes our results essentially polarization-independent, whereas the use of a thin film restricts the enhancement to a single polarization. We report the enhancement of tunneling probability, not extinction ratio, since our enhancement is so large that it takes the modes from undercoupled, through critical coupling, to overcoupled. For comparison, an estimate using our analysis applied to some results presented in [18] yields $F_c = 8.0$, $F_i = 1.7$. Our greater coupling enhancement probably reflects the greater SP field enhancement at the surfaces of nanoparticles.

Gold-nanorod-coated microresonators are expected to enhance the sensitivity of WGM evanescent-wave chemical sensors. These resonators are also good candidates for surface-enhanced Raman scattering experiments. Device fabrication is being investigated.

Acknowledgements This work was supported by the National Science Foundation under Award Nos. ECCS-0601362, ECS-0329924, and EPS-0132534, by the Oklahoma State Regents for Higher Education, and by the Oklahoma Center for the Advancement of Science and Technology under Award No. AR072-066. The authors thank Dr. N.A. Kotov for supplying the HgTe NPs, and Drs. B.N. Flanders, J.P. Wicksted, and J.J. Martin for assistance.

References

1. E. Kretschmann, H. Raether, Z. Naturforsch. A: Phys. Sci. A **23**, 2135 (1968)
2. W.H. Weber, S.L. McCarthy, Appl. Phys. Lett. **25**, 396 (1974)
3. R.H. Ritchie, E.T. Arakawa, J.J. Cowan, R.N. Hamm, Phys. Rev. Lett. **21**, 1530 (1968)
4. I. Pockrand, J. Phys. D **9**, 2423 (1976)
5. G. Schider, J.R. Krenn, W. Gotschy, B. Lamprecht, H. Ditlbacher, A. Leitner, F.R. Aussenegg, J. Appl. Phys. **90**, 3825 (2001)
6. E. Kretschmann, Opt. Commun. **10**, 353 (1974)
7. W. Lukosz, Biosens. Bioelectron. **6**, 215 (1991)
8. R.D. Harris, J.S. Wilkinson, Sens. Actuators B **29**, 261 (1995)
9. P. Stöcker, B. Menges, U. Langbein, S. Mittler, Sens. Actuators A **116**, 224 (2004)
10. A.K. Sharma, R. Jha, B.D. Gupta, IEEE Sens. J. **7**, 1118 (2007)
11. J.N. Yih, F.-C. Chien, C.-Y. Lin, H.-F. Yau, S.-J. Chen, Appl. Opt. **44**, 6155 (2005)
12. G.C. Papavassiliou, Prog. Solid State Chem. **12**, 185 (1979)
13. D. Amarie, T.-D. Onuta, R.A. Potyrailo, B. Dragnea, J. Phys. Chem. B **109**, 15515 (2005)
14. K.A. Fuller, D.D. Smith, Opt. Express **15**, 3575 (2007)
15. S.I. Shopova, C.W. Blackledge, A.T. Rosenberger, N.F. Materer, Appl. Phys. Lett. **89**, 023120 (2006)
16. A.T. Rosenberger, Opt. Express **15**, 12959 (2007)
17. S.I. Shopova, PhD dissertation, Oklahoma State University, 2007
18. N.K. Hon, A.W. Poon, J. Opt. Soc. Am. B **24**, 1981 (2007)